An active vibration control strategy for a flexible link using distributed ionic polymer metal composites

ARTICLE *in* SMART MATERIALS AND STRUCTURES · MARCH 2007

Impact Factor: 2.5 · DOI: 10.1088/0964-1726/16/3/008

3 AUTHORS, INCLUDING:

Bishakh Bhattacharya
Indian Institute of Technology Kanpur
62 PUBLICATIONS **150** CITATIONS
SEE PROFILE

Ashish Dutta
Indian Institute of Technology Kanpur
56 PUBLICATIONS **163** CITATIONS
SEE PROFILE

Smart Mater. Struct. **16** (2007) 617–625 doi:10.1088/0964-1726/16/3/008

An active vibration control strategy for a flexible link using distributed ionic polymer metal composites

Dibakar Bandopadhya, Bishakh Bhattacharya and Ashish Dutta

Department of Mechanical Engineering, IIT Kanpur, Kanpur-208016, India

E-mail: dibakarb@iitk.ac.in, bishakh@iitk.ac.in and adutta@iitk.ac.in

Received 22 May 2006, in final form 19 January 2007
Published 16 March 2007
Online at stacks.iop.org/SMS/16/617

Abstract
Ionic polymer metal composites are a class of electro-active polymers that are gaining importance as smart actuators due to their large bending deflection. The property of generating high strains with low actuation voltage makes ionic polymer metal composites (IPMC) suitable for applications requiring large motion such as in large deflection vibration suppression. In this paper we propose an application of IPMC as an active damper for large deflection vibration control of a flexible link. The modes of vibration for a long flexible link are derived using the modal approach and two IPMC patches are placed to suppress the vibration. A distributed PD controller is designed to suppress the vibration of the flexible link for the desired positioning of the tip. Simulations are first done to demonstrate effective vibration suppression and the results proved that the proposed method can suppress vibration effectively. Experiments are conducted to verify the application of IPMC for active vibration suppression. The performance of the proposed distributed PD controller is also found to be better than a single PD controller loop.

(Some figures in this article are in colour only in the electronic version)

1. Introduction

The property of producing large bending moment and active strain by relatively low actuating voltage has made IPMC attractive for both active and hybrid (strain-dependent) damping applications. Performance of a flexible link is always limited by the generation of parasitic vibration due to its low stiffness. Various passive, active and combined damping schemes have been proposed in the past to restrain such vibration within desired limits. Smart piezoelectric materials have been used successfully for controlling vibration of a single link and multi-link system [1–3]. The piezoelectric actuators are modeled as a coupled system integrated with the host link. Application of control voltage in such piezoelectric actuators is shown to generate end moments about the neutral axis of the link at the two end points of the actuator [4]. Often due to the limitations of availability of high power, active constraint layer strategies are adopted wherein the frequency-dependent viscoelastic layers are actively deformed by piezoelectric layers. It is observed that about 5% damping factor could be achieved for a flexible link of slenderness ratio about 120 [5]. Similar strategies are adopted while controlling vibration using a magnetostrictive (Terfenol-D) actuator. Here the active strain is generated by a changing magnetic field around the smart actuator. A combined passive and active damping scheme using a combination of layers of ferromagnetic (passive) and smart (active) magnetostrictive material in hybrid mode has been proposed to control vibration [6]. In comparison to the piezoelectric material mostly used, electro-active polymers require control voltages of around 3–5 V while piezoelectric actuators normally require around 200–500 V. This eliminates the extra mass associated with power electronics, making ionic polymers a lightweight alternative. Also due to high brittleness, PZT actuators are manufactured in relatively small dimensions and may lead to breakdown under fatigue loading. An advantage of ionic polymers over PVDF is that they are more compliant and sensitive to the change of applied strain.

Electro-active polymers (EAP) are a class of active materials that are classified into two categories: electronic,

driven by electric field, and ionic, driven by diffusion of ions [7, 8]. Ionic polymer material has both fixed anions and mobile cations. The electromechanical coupling in ionic polymers is ionic diffusion, specifically the motion of mobile cations. When the material is hydrated the cations diffuse toward an electrode on the material surface under an applied electric field. Inside the polymer structure, anions are interconnected as clusters providing channels for the cations to flow towards the electrode. This motion of ions causes the structure to bend toward the anode [9, 10]. The extremely large motion relative to size makes the polymers attractive as actuators. Also, EAPs only require a few volts for actuation, usually less than 5 V [11–14]. IPMCs are generally manufactured with an ionic polymer (nafion) with ion exchanging capability which is then chemically treated with an ionic salt, namely perfluorinated polymer electrolyte solution sandwiched by platinum or gold electrodes on both sides [15–19].

The main objectives of this paper are to study the use of IPMC for active vibration suppression of a flexible link. The studies are directed:

(a) to use IPMC as an active damper for large deflection flexible link;
(b) to design a distributed PD controller for actuating IPMC patches on a flexible link;
(c) to compare the performance of control of a single-loop PD controller with the proposed two-loop distributed PD controller.

The proposed technique utilizes the property that, under a control input voltage, IPMC bonded onto the flexible link bends and generates a distributed bending moment that opposes the structural vibration. Initially the three major modes of vibration for the flexible link are determined and then, based on the position of the two modes, two IPMC strips are placed on the base material. Piezoelectric (bimorph) sensors are placed behind each IPMC and are used to record the strain amplitude of vibration of the cantilever link for different magnitudes of disturbance applied to the link. A distributed PD controller is designed to suppress the vibrations by actuating the IPMC to balance the vibrations. In section 2 properties of IPMC are briefly discussed which give the relationship between curvature with input voltage. Section 3 presents the modeling of the flexible link used to obtain the modes of vibration and according to which IPMC patches are placed. In section 4 integrated dynamic models of flexible link and IPMC patches are formulated. Simulation results are given in section 5. A distributed PD controller is designed as an active controller in section 6, followed by experimental results and discussions in section 7. Finally the conclusion is drawn in section 8.

2. Mechanical properties

In order to obtain the voltage versus curvature relationship, a strip of IPMC of size 35 × 10 × 0.5 (mm) has been tested in cantilever mode. Copper strips are used at each end and the voltage is applied quasi-statically from a DC power supply (0–60 V, 0–10 A, supplied by Elnova Ltd, New Delhi). Subsequently the bending of IPMC is recorded through graph

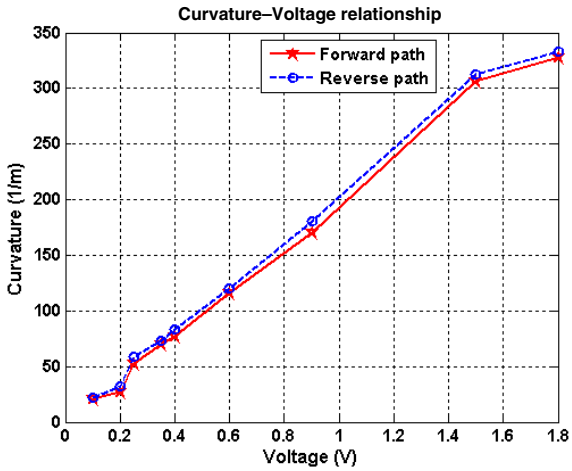

Figure 1. Voltage versus curvature relationship obtained experimentally for the IPMC used in the experiment.

paper for each input voltage. The end deflection δ of the beam of length L due to an input voltage V can be related approximately to the radius of curvature R as

$$R = \frac{1}{\kappa} \cong \frac{L^2 + \delta^2}{2\delta} \tag{1}$$

where κ is the curvature of the IPMC strip. After measuring the deflection in IPMC against the applied voltage experimentally, the above relationship is used to obtain the voltage versus curvature relationship and plotted in figure 1. It is understood from figure 1 that the voltage–curvature relationship remains mostly linear for both increasing and decreasing voltages. Therefore, one can assume the curvature voltage relationship as

$$\kappa = K \times V + \kappa_{0.1} \qquad 0.1 \leqslant V \leqslant 1.8 \tag{2}$$

where κ = curvature, K is a path constant, which can be determined from the experimental data, and V = applied voltage. The value of K depends on the backbone materials, counter ions and its amount and the property of the solvent present. Using equation (2) we can express the relation between bending moment and applied voltage as

$$M_{\mathrm{b}} = \frac{EI}{R} = \frac{1}{12} \times K \times E \times V \times w_i \times h^3 \tag{3}$$

where M_{b} = bending moment generated, E = modulus of elasticity, w_i = width of the IPMC and h is the thickness of the IPMC strip/patch. Figure 2 shows the bending moment variation with input voltage varying along the width of the strip.

The bending moment generated depends significantly on the moisture content and thus movement of ions within IPMC from the backbone materials. The metallization of the top and bottom surface of IPMC acts as electrodes. These are quite thin, of the order of 1–4 μm, and hence do not affect the modulus of elasticity of the IPMC significantly.

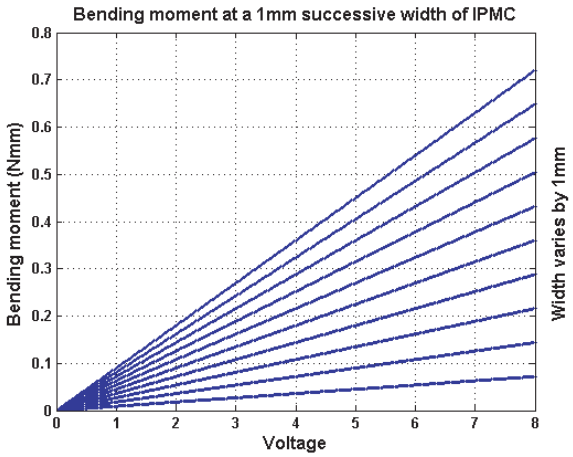

Figure 2. Bending moment and voltage relationship along the width of the IPMC.

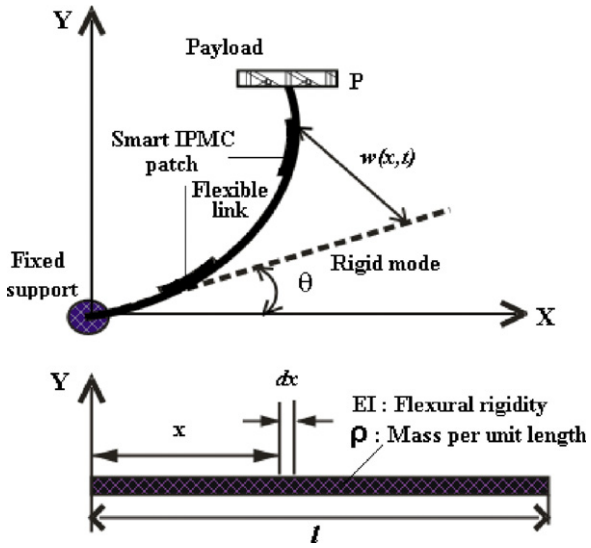

Figure 3. Flexible link configuration.

3. Modeling of a flexible link with IPMC

3.1. Modes and modal properties

A flexible link is modeled as a continuous distributed parameter system. Let w represent the bending displacement at any location x, ρ the mass per unit length and EI the flexural rigidity of the link. Then the equation for free vibration of the link shown in figure 3 is given by

$$EI\left(\frac{\partial^4 w}{\partial x^4}\right) = -\rho\frac{\partial^2 w}{\partial t^2}. \tag{4}$$

Assuming that the solution of equation (4) is separable in time and space, i.e.

$$w(x,t) = \varphi(x)q(t) \tag{5}$$

$$\phi(x) = A_1\sin(\beta x) + A_2\cos(\beta x) + A_3\sin(h\beta x) + A_4\cos(h\beta x) \tag{6}$$

where the constant coefficients A_1, A_2, A_3, A_4 and the parameter β are to be determined by using boundary conditions.

3.2. Boundary conditions

Consider one end of the link is clamped and the other is free. At the clamped end, $x = 0$, the bending displacement and its slope are zero, and thus boundary conditions are

$$\varphi(0) = 0, \qquad \left.\frac{\mathrm{d}\varphi(x)}{\mathrm{d}x}\right|_{x=0} = 0. \tag{7}$$

At the free end, $x = l$, the external moment and shear force are zero and thus the boundary conditions are

$$\left.\frac{\mathrm{d}^2\varphi(x)}{\mathrm{d}x^2}\right|_{x=l} = 0, \qquad \left.\frac{\mathrm{d}^3\varphi(x)}{\mathrm{d}x^3}\right|_{x=l} = 0. \tag{8}$$

This gives the characteristic equation equality

$$\cos\beta l\cosh\beta l = -1. \tag{9}$$

Equation (9) is commonly referred to as the characteristic fundamental frequency equation of a cantilevered uniform flexible link. It has an infinite number of solutions for β_k, $k = 1, 2, \ldots, \alpha$ that can be obtained only numerically. The first three values of βl and corresponding frequency formulae are given by [20]

$$\beta_1 l = 1.8751 \Rightarrow \omega_1 = 1.8751^2\sqrt{\frac{EI}{\rho l^4}},$$

$$\beta_2 l = 4.6941 \Rightarrow \omega_2 = 4.6941^2\sqrt{\frac{EI}{\rho l^4}},$$

$$\beta_3 l = 7.8548 \Rightarrow \omega_3 = 7.8548^2\sqrt{\frac{EI}{\rho l^4}}.$$

The quantities ω_k $(k = 1, 2, \ldots, \alpha)$ are called characteristic values or eigenvalues. They are also known as natural frequencies. In figure 4 it is shown that the first two modes take the maximum amount of energy and on incrementing of mode numbers, total energy does not change appreciably. Based on

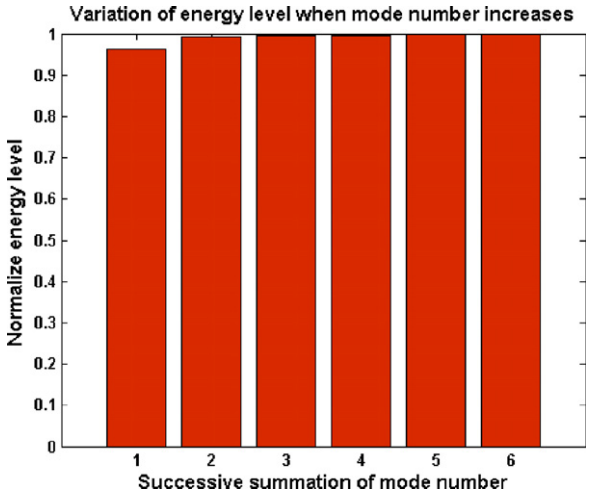

Figure 4. Successive summation of total energy as mode number increases up to six.

this we have considered to use two strips of IPMC as actuators, as it will be satisfactory for suppression of the two major modes of vibration. This will also minimize the cost of the IPMC being used.

4. Dynamic modeling of the flexible link

4.1. Kinetic energy of the system

Velocity at any point at a distance x on the link can be expressed as

$$v = x\dot{\theta} + \dot{w} \tag{10}$$

where θ is the angle between the vibratory link and the mean axis. The kinetic energy of the system is the sum of the kinetic energy of the flexible link and kinetic energy of the payload. The velocities at each point on the link depend on the position and time. A similar dynamic modeling has been reported in [4, 21]. The kinetic energy of the link at any instant is given by

$$\begin{aligned} T_l &= \tfrac{1}{2}\int_0^l \rho\left(x\dot{\theta} + \dot{w}\right)^2 \mathrm{d}x \\ &= \frac{\rho}{2}\int_0^l \left(x^2\dot{\theta}^2 + 2x\dot{\theta}\dot{w} + \dot{w}^2\right) \mathrm{d}x \end{aligned} \tag{11}$$

$$\begin{aligned} T_l &= \frac{\rho}{2}\int_0^l x^2\dot{\theta}^2\,\mathrm{d}x + \rho\int_0^l x\dot{\theta}\dot{w}\,\mathrm{d}x + \frac{\rho}{2}\int_0^l \dot{w}^2\,\mathrm{d}x \\ &= \frac{\rho}{2}\frac{l^3}{3}\dot{\theta}^2 + \rho\int_0^l \varphi(x)\dot{q}(t)\dot{\theta}\,\mathrm{d}x + \frac{\rho}{2}\int_0^l \varphi(x)^2\dot{q}^2\,\mathrm{d}x. \end{aligned}$$

Kinetic energy due to payload is given by

$$\begin{aligned} T_\mathrm{p} &= \frac{1}{2}M_\mathrm{p}[\dot{r}(l)]^2 = \frac{M_\mathrm{p}}{2}\left[l\dot{\theta} + \dot{w}\right]^2 \\ &= \frac{M_\mathrm{p}}{2}l^2\dot{\theta}^2 + M_\mathrm{p}l\dot{\theta}\varphi(l)\dot{q} + \frac{M_\mathrm{p}}{2}\varphi(l)^2\dot{q}^2. \end{aligned} \tag{12}$$

Therefore, the total kinetic energy is given by

$$\begin{aligned} T &= T_l + T_\mathrm{p} \\ &= \frac{\rho}{2}\frac{l^3}{3}\dot{\theta}^2 + \rho\int_0^l \varphi(x)\dot{q}(t)\dot{\theta}\,\mathrm{d}x + \frac{\rho}{2}\int_0^l \varphi(x)^2\dot{q}^2\,\mathrm{d}x \\ &\quad + \frac{M_\mathrm{p}}{2}l^2\dot{\theta}^2 + M_\mathrm{p}l\dot{\theta}\varphi(l)\dot{q} + \frac{M_\mathrm{p}}{2}\varphi(l)^2 \end{aligned}$$

$$\begin{aligned} T &= \frac{1}{2}\left\{\rho\frac{l^3}{3} + M_\mathrm{p}l^2\right\}\dot{\theta}^2 \\ &\quad + \left\{M_\mathrm{p}l\varphi(l) + \rho\int_0^l \varphi(x)\,\mathrm{d}x\right\}\dot{\theta}\dot{q} \\ &\quad + \tfrac{1}{2}\left[M_\mathrm{p}\varphi(l)^2 + \int_0^l \varphi(x)^2\,\mathrm{d}x\right]\dot{q}^2. \end{aligned} \tag{13}$$

Letting

$$\begin{aligned} M_{TT} &= \left\{\rho\frac{l^3}{3} + M_\mathrm{p}l^2\right\}, \\ M_{TQ} &= M_\mathrm{p}l\varphi(l) + \rho\int_0^l \varphi(x)\,\mathrm{d}x, \\ M_{QQ} &= M_\mathrm{p}\varphi(l)^2 + \int_0^l \varphi(x)^2\,\mathrm{d}x \\ T &= \tfrac{1}{2}M_{TT}\dot{\theta}^2 + M_{TQ}\dot{\theta}\dot{q} + \tfrac{1}{2}M_{QQ}\dot{q}^2. \end{aligned} \tag{14}$$

4.2. Potential energy

The potential energy of the system is due to deformation of the link, payload and its own weight. It is assumed that the link's own weight acts as a point mass with the payload and the link deformation is also dependent on the position of the link and time. Hence the potential energy of the link is given by

$$V_1 = \tfrac{1}{2}\int_0^l E_\mathrm{b}I_\mathrm{b}\left(w''(x,t)\right)^2\,\mathrm{d}x \tag{15}$$

where E_b = modulus of elasticity and I_b = area moment of inertia of the link. $w''(x,t)$ = double differentiation of w with respect to x. Now

$$w''(x,t) = \frac{\mathrm{d}^2}{\mathrm{d}x^2}w(x,t) = \frac{\mathrm{d}^2}{\mathrm{d}x^2}\left(\varphi(x)q(t)\right) = \varphi''(x)q(t).$$

Therefore,

$$\begin{aligned} V_1 &= \tfrac{1}{2}\int_0^l E_\mathrm{b}I_\mathrm{b}\left(\varphi''(x)q(t)\right)^2\,\mathrm{d}x \\ &= q^\mathrm{T}\left[\tfrac{1}{2}\int_0^l E_\mathrm{b}I_\mathrm{b}\left(\varphi''(x)\right)^2\,\mathrm{d}x\right]q. \end{aligned} \tag{16}$$

This can be written as

$$V_1 = \tfrac{1}{2}q^\mathrm{T}K_q q \tag{17}$$

where

$$K_q(i,j) = \tfrac{1}{2}\int_0^l E_\mathrm{b}I_\mathrm{b}\varphi_i''(x)\varphi_j''(x)\,\mathrm{d}x.$$

The potential energy due to payload (assumed as a point mass) is given by $V_2 = M_\mathrm{p}gz$, where, $z = l\theta(t) + \varphi(l)q(t)$. Using this we get the potential energy due to payload

$$V_2 = M_\mathrm{p}g\left[l\theta(t) + \varphi(l)q(t)\right]. \tag{18}$$

Hence total potential energy of the system is given by

$$V = \tfrac{1}{2}q^\mathrm{T}K_q q + M_\mathrm{p}g\left[l\theta(t) + \varphi(l)q(t)\right]. \tag{19}$$

4.3. Work done due to input torque and IPMC patches

Work done due to IPMC actuators can be expressed as

$$\delta W = \int_0^l M(x,t)\tfrac{1}{2}bd\left(\delta\theta + \varphi'(x)\delta\dot{q}\right)\,\mathrm{d}x \tag{20}$$

where b is the width of the link, and d is the thickness of the link. Considering perfectly bonded IPMC actuators the above equation can be written as

$$\begin{aligned} \delta W &= \sum_{i=1}^{n}\delta W_i = \sum_{i=1}^{n}M_{\mathrm{b}i}\delta\theta + \sum_{i=1}^{n}M_{\mathrm{b}i}[H(x-x_i) \\ &\quad - H(x-x_{i+1})][\varphi'(x_{i+1}) - \varphi'(x_i)]\delta\dot{q}\sin^2(\mathrm{i}\pi/2) \end{aligned}$$

where $M_{\mathrm{b}i}$ is the bending moment generated by the IPMC active layer. $[H(x-x_i) - H(x-x_{i+1})]$ is the *Heaviside* function with value 1 or 0 according to the discontinuity of the actuator placement. $[H(x-x_i) - H(x-x_{i+1})] = 1$ for continuous patch and 0 for areas without patches. The term $[\varphi'(x_{i+1}) - \varphi'(x_i)]\delta\dot{q}$ denotes the slope difference between two ends of the ith actuator (patch). For uniformly distributed IPMC patch the value of the *Heaviside* function must be '1',

Table 1. Material properties of both link material and IPMC.

Property	Aluminum	IPMC
Elastic modulus (GPa)	70	1.2
Length	0.8 m	40 mm
Width (mm)	50	10
Thickness (mm)	4	0.2
Area of c/s (mm^2)	200	2
Density (kg m^{-3})	2700	2000

i.e. $[H(x-x_i)-H(x-x_{i+1})] = 1$. Therefore the above expression is reduced to

$$\delta W = \sum_{i=1}^{n} \delta W_i = \sum_{i=1}^{n} M_{bi}\delta\theta + \sum_{i=1}^{n} M_{bi}\left[\varphi'(x_{i+1}) - \varphi'(x_i)\right]\delta\dot{q}. \tag{21}$$

Again, if we assume that bending moment generated by each patch of the same dimension is equal then the above equation is simplified to

$$\delta W = M_{\text{bt}}\delta\theta + M_{\text{bt}}\left[\varphi'(a_2) - \varphi'(a_1)\right]\delta\dot{q} \tag{22}$$

where M_{bt} is the total bending moment generated by n patches of IPMC and $(a_2 - a_1)$ represents the IPMC coverage.

4.4. Equation of motion

Using Hamiltonian formulation we have

$$\int_{t_0}^{t_f} (\delta T - \delta V + \delta W)\, \mathrm{d}t = 0$$

$$\begin{aligned}
\delta T &= M_{TT}\dot{\theta}\delta\dot{\theta} + M_{TQ}\dot{\theta}\delta\dot{q} + M_{TQ}\dot{q}\delta\dot{\theta} + M_{QQ}\dot{q}\delta\dot{q} \\
\delta V &= K_q q\delta q + M_{\text{p}} g\left[l\delta\theta + \varphi(l)\delta q\right] \\
&= \left[K_q q + M_{\text{p}} g\varphi(l)\right]\delta q + M_{\text{p}} gl\delta\theta
\end{aligned} \tag{23}$$

and $\delta W = M_{\text{bt}}\delta\theta + M_{\text{bt}}[\varphi'(a_2) - \varphi'(a_1)]\delta\dot{q}$.

Therefore, on integration, equation (23) is simplified to

$$\begin{aligned}
&\int_{t_0}^{t_f} (\delta T_{\text{total}} - \delta V + \delta W)\, \mathrm{d}t \\
&= -\int_{t_0}^{t_f} \left(M_{TT}\ddot{\theta} + M_{TQ}\ddot{q}\right)\delta\theta\, \mathrm{d}t \\
&\quad - \int_{t_0}^{t_f} \left(M_{TQ}\ddot{\theta} + M_{QQ}\ddot{q}\right)\delta q\, \mathrm{d}t \\
&\quad - \int_{t_0}^{t_f} \left[\left\{K_q q + M_{\text{p}} g\varphi(l)\right\}\delta q + M_{\text{p}} gl\delta\theta\right]\mathrm{d}t \\
&\quad + \int_{t_0}^{t_f} M_{\text{bt}}\delta\theta\, \mathrm{d}t = 0.
\end{aligned}$$

Grouping all the terms containing $\delta\theta$ and δq separately we get

$$\begin{aligned}
&-\int_{t_0}^{t_f} \left\{M_{TT}\ddot{\theta} + M_{TQ}\ddot{q} + M_{\text{p}} gl - M_{\text{bt}}\right\}\delta\theta\, \mathrm{d}t \\
&\quad - \int_{t_0}^{t_f} [(M_{TQ}\ddot{\theta} + M_{QQ}\ddot{q}) \\
&\quad + (K_q q + M_{\text{p}} g\varphi(l))]\delta q\, \mathrm{d}t = 0.
\end{aligned} \tag{24}$$

Separating rigid and flexible modes we get the equation of motion as

$$\begin{aligned}
M_{TT}\ddot{\theta} + M_{TQ}\ddot{q} + M_{\text{p}} gl - M_{\text{bt}} = 0 \\
M_{TQ}\ddot{\theta} + M_{QQ}\ddot{q} + K_q q + M_{\text{p}} g\varphi(l) = 0.
\end{aligned} \tag{25}$$

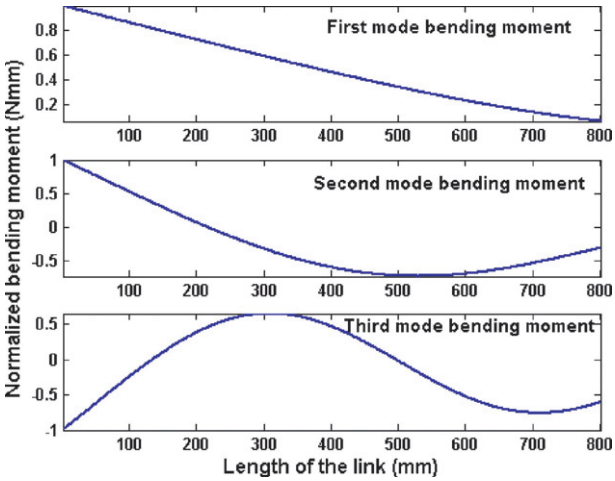

Figure 5. Bending moment variation for first three modes of the flexible link of length 80 cm.

Arranging this into the matrix form we get

$$\begin{bmatrix} M_{TT} & M_{TQ} \\ M_{TQ} & M_{QQ} \end{bmatrix}\begin{bmatrix} \ddot{\theta} \\ \ddot{q} \end{bmatrix} + \begin{bmatrix} 0 \\ K_q \end{bmatrix}\begin{bmatrix} \theta \\ q \end{bmatrix} = \begin{bmatrix} M_{\text{bt}} - M_{\text{p}} gl \\ -M_{\text{p}} g\varphi(l) \end{bmatrix}. \tag{26}$$

A special case when there is no payload the above equation is reduced to

$$\begin{bmatrix} M_{TT} & M_{TQ} \\ M_{TQ} & M_{QQ} \end{bmatrix}\begin{bmatrix} \ddot{\theta} \\ \ddot{q} \end{bmatrix} + \begin{bmatrix} 0 \\ K_q \end{bmatrix}\begin{bmatrix} \theta \\ q \end{bmatrix} = \begin{bmatrix} M_{\text{bt}} \\ 0 \end{bmatrix}. \tag{27}$$

5. Simulation results

In this section, the results obtained from numerical simulation using the link and IPMC properties are shown in table 1 for a known vibration source. All programs are developed in MATLAB. To solve the differential equations in state space, a function of MATLAB called '*Ode45' is* used. Ode45 is based on a fourth-and fifth-order Runge–Kutta scheme with adaptive step size.

5.1. Damping scheme

Figure 5 shows the bending moment variation of the flexible link for the first three modes of vibration. Based on this the position of the two IPMC actuators have been located on the link, to suppress the first and second mode of vibration. IPMC actuators have been placed as shown in figure 3 which is clamped at one end.

Figures 6 and 7 show the undamped and damped response of the flexible beam for cosine torque input as disturbance. It is observed that using two patches IPMC as an active damper tip deflection of the link can be reduced up to 80%.

Figure 8 is showing the variation of tip slope during damping while figure 9 shows the reduction in tip deflection corresponding to cosine torque input which is around 80%. It may be noted that there are intermittents possibly of large amplitude due to nonlinearity in the system.

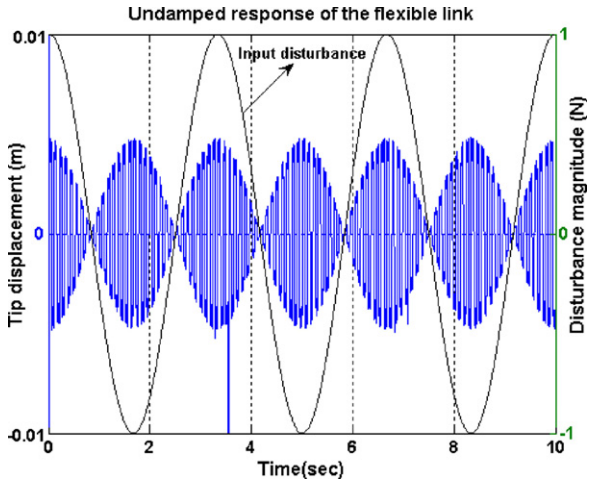

Figure 6. Undamped response of the flexible link for cosine torque input as disturbance.

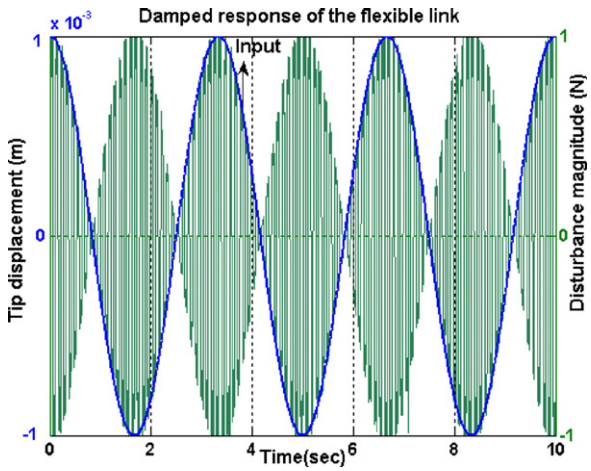

Figure 7. Damped response of the flexible link for cosine torque input as disturbance.

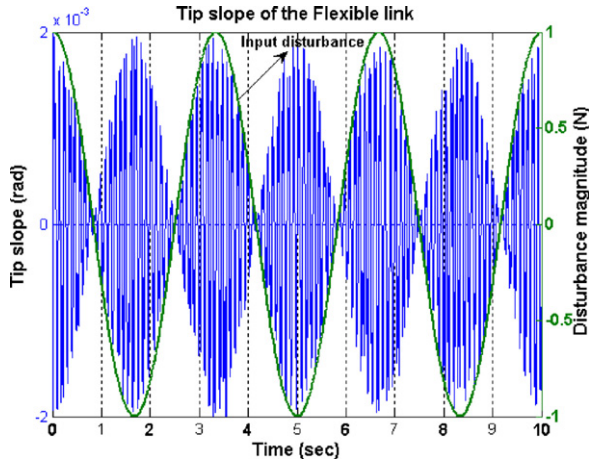

Figure 8. Tip slope of the flexible link for cosine torque input as disturbance.

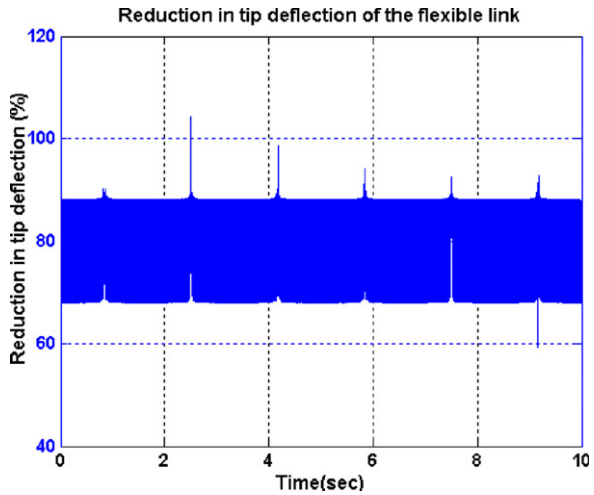

Figure 9. Reduction in tip deflection of the flexible link.

6. Design of distributed PD controller

The equation of motion of the flexible link takes the form

$$M_m\ddot{x} + C_{\mathrm{d}}\dot{x} + K_s x = Bu \tag{28}$$

where M_m and K_s are symmetric matrices for a flexible link. The system of equations can be transformed into new coordinates that are convenient. Employing a proportional damping scheme one can write the damping matrix as

$$C = \alpha_1 M_m + \alpha_2 K_s \tag{29}$$

where α_1, α_2 are the constants. Further considering linear transformation one can take

$$x = \Phi\lambda \Rightarrow \lambda = \Phi^{-1}x \tag{30}$$

where Φ is the orthonormal modal matrix with respect to M_m and K_s. λ is the normal principal coordinate. The orthonormal modal matrix converts symmetric coupled modal mass and stiffness matrix into diagonal matrices, thus decoupling the system for each mode which makes the controller design simple and straightforward. Substituting new coordinates into equation (28) we get

$$M_m\Phi\ddot{\lambda} + C_{\mathrm{d}}\Phi\dot{\lambda} + K_s\Phi\lambda = Bu. \tag{31}$$

Multiplying both sides by Φ^{T}, we get

$$\Phi^{\mathrm{T}}M_m\Phi\ddot{\lambda} + \Phi^{\mathrm{T}}C_{\mathrm{d}}\Phi\dot{\lambda} + \Phi^{\mathrm{T}}K_s\Phi\lambda = \Phi^{\mathrm{T}}Bu. \tag{32}$$

Let us consider

$$\Phi^{\mathrm{T}}M_m\Phi = \bar{M}_m, \qquad \Phi^{\mathrm{T}}C_{\mathrm{d}}\Phi = \bar{C}_{\mathrm{d}},$$

$$\Phi^{\mathrm{T}}K_s\Phi = \bar{K}_s, \qquad \phi^{\mathrm{T}}B = \bar{B}.$$

as the new modal mass, damping, stiffness and input matrices, respectively, in terms of the modal coordinates. Therefore, the modified equation can be written as

$$\bar{M}_m\ddot{\lambda} + \bar{C}_{\mathrm{d}}\dot{\lambda} + \bar{K}_s\lambda = \bar{B}u. \tag{33}$$

Now, $\Phi^{\mathrm{T}}M_m\Phi = \bar{M}_m = I$, $\Phi^{\mathrm{T}}K_s\Phi = \bar{K}_s = \Psi$ where Ψ is a diagonal matrix with diagonal elements $\omega_1^2, \omega_2^2, \ldots, \omega_n^2$.

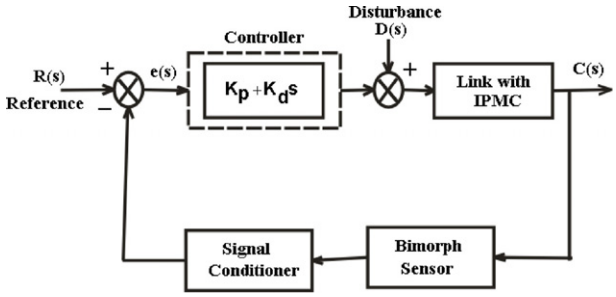

Figure 10. Schematic diagram of proportional derivative controller with plant.

Introducing a column input vector $\bar{u}(t)$ associated with the coordinate vector q and related to the input vector $u(t)$, i.e. $\bar{u}(t) = \bar{B}u$, the modified equation of motion in the new coordinate system can be expressed as

$$\ddot{\lambda}(t) + \bar{C}_{\mathrm{d}}\dot{\lambda}(t) + \Psi\lambda(t) = \bar{u}(t). \tag{34}$$

The controlled system is shown in figure 10. Taking into account the damping and then on the Laplace transform

$$\left(s^2 + 2\zeta\omega s + \omega^2\right)\lambda(s) = \bar{u}(s) \Rightarrow \frac{\lambda(s)}{\bar{u}(s)} = \frac{1}{s^2 + 2\zeta\omega s + \omega^2}$$

is the transfer function of the system, where ζ is the damping coefficient. Considering a PD compensator $K_{\mathrm{p}} + K_{\mathrm{d}}s$, the open loop transfer function of the system can be written as

$$\frac{K_{\mathrm{p}} + K_{\mathrm{d}}s}{\left(s^2 + 2\zeta\omega s + \omega^2\right)} \tag{35}$$

where K_{p} is the proportional gain and K_{d} is the derivative gain. Taking positive feedback, the response $C(s)$ due to the simultaneous application of the reference input $R(s)$ and disturbance $D(s)$ is given by

$$\begin{aligned} C(s) &= \frac{C_R(s)}{R(s)} + \frac{C_D(s)}{D(s)} \\ &= \frac{1 + K_{\mathrm{p}} + K_{\mathrm{d}}s}{s^2 + (2\zeta\omega + K_{\mathrm{d}})s + (\omega^2 + K_{\mathrm{p}})}. \end{aligned} \tag{36}$$

Figure 10 shows the schematic of the distributed PD control system employed in our active control strategy.

7. Experimental results

7.1. IPMC as active damper for known vibration source

In the experimental test set-up, a flexible link of 0.8 m made of aluminum as a host link is tested. Two bimorph piezoelectric sensors are mounted on the link collocated with the IPMC to develop two independent control loops from the base of the test specimen's fixed end. PC interfacing of bimorph data is carried out through DAQ-PCI-6251 and NI-DAQmx devices (supplied by National Instrumentation) with signal conditioner. The test specimen is excited by a vibration generator of type SP2 supplied by Spranktronics, Bangalore. The bimorph signal is sensed and based on it the IPMC is actuated so as to oppose the vibration. The following are the control parameters:

Amplifier gain: 10;

Figure 11. Experimental set-up is showing two IPMC patches on the link and the exciter.

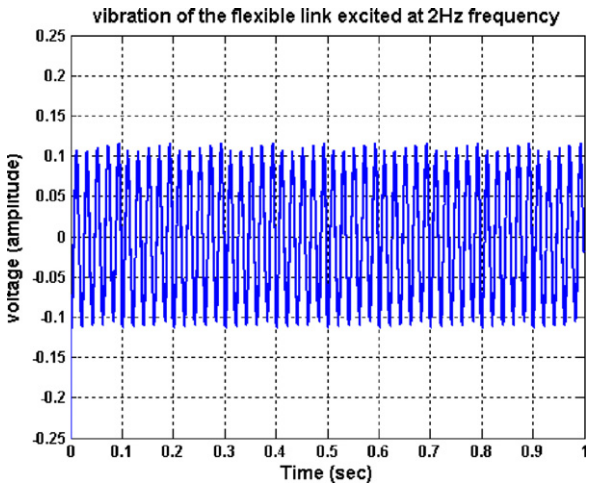

Figure 12. Forced vibration of flexible link at 2 Hz frequency.

Excitation voltage: 5 V;

Actuator current amplitude: 167 mA.

Figure 11 shows the experimental set-up of the active control strategy employed for a known vibration source used to study the damping characteristics.

Figure 12 is showing undamped vibration of the link at 2 Hz frequency. Figure 13 shows the corresponding damped response of vibration of the link. Here amplitude is shown in terms of voltage representing strains generated in IPMC due to deflection of the flexible link. It is observed that two patches of IPMC have reduced the vibration around 75% quantitatively. Details are reported in [22]. Experimentally it has been verified that the voltage generated in the bimorph sensor is proportional to the tip deflection of the flexible link.

7.2. IPMC as active damper for unknown vibration source

For unknown vibration source, as is done earlier the same distributed PD controller is used to attenuate the vibration of the flexible link for desired positioning of the tip. Two IPMC patches are placed on the flexible link collocated with the sensors. Sensor 1 and 2 are placed 0.3 and 0.6 m away from the clamped end of the link, respectively. Impact force of 0.0981 N is used to vibrate the link of the same length. It is observed that a distributed PD controller integrated with IPMC

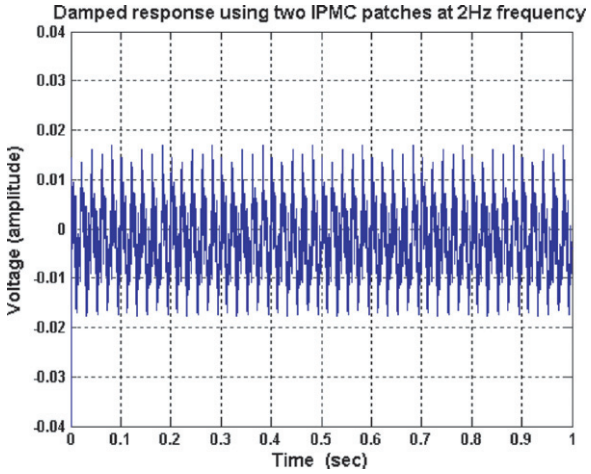

Figure 13. Damped vibration response of flexible link using two patches of IPMC at 2 Hz frequency.

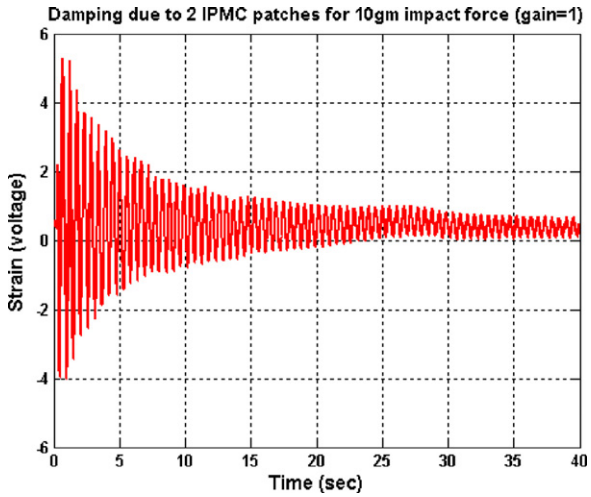

Figure 14. Damping due to single-loop PD controller using two patches of IPMC.

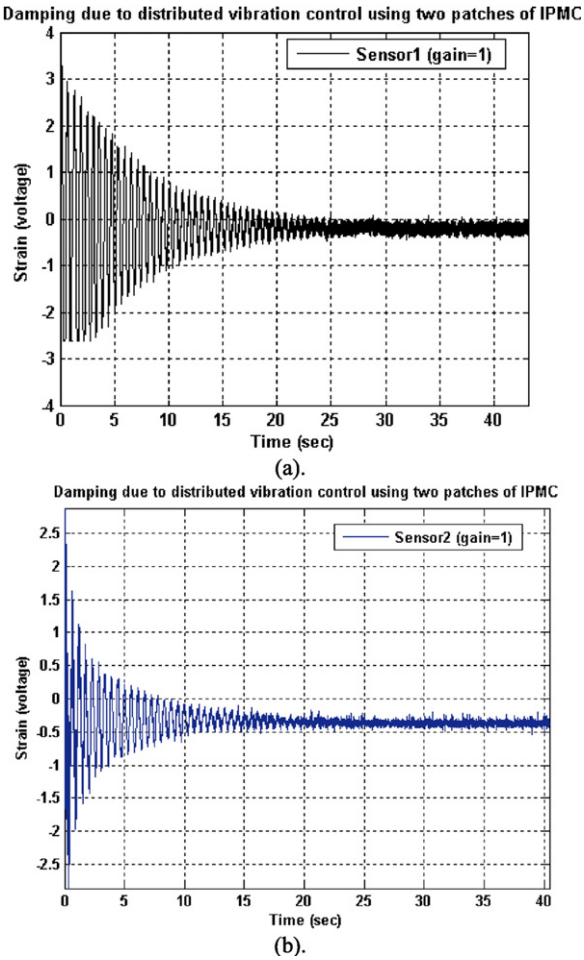

Figure 15. The damping response for sensor 1 and sensor 2, respectively, due to two independent PD controller loops.

attenuates the vibration considerably. Figure 14 is showing the damped response of the single-loop PD controller using two IPMC patches while figure 15 is showing the damped response due to two independent distributed PD controllers using two IPMC patches. It is observed that the distributed PD controller performed better in vibration attenuation over a single-loop PD controller under the same impact force of 0.0981 N and end condition.

From figure 15 it is observed that at sensor 2 damping is a little faster than at sensor 1, since the effectiveness of actuator 2 is better than actuator 1. It is also observed that a two-loop independent distributed PD controller attenuates the vibration faster than a single-loop PD controller. Offset is present due to the initial displacement of the link from its mean position due to its self-weight. It is observed that a damping factor of 5–8% could be achieved by using two patches of IPMC.

8. Conclusion

It has been shown both analytically and experimentally that an IPMC based distributed control scheme can effectively suppress vibration in a flexible link. It is observed that a two-loop distributed PD controller gives better results than a single-loop PD controller to suppress the vibration. Further incrementing IPMC patches or length of the patches, each with an independent PD controller, would be a good alternative to suppress the high amplitude vibration. This would, of course, increase the cost of the control. As future work we hope to carry out the vibration suppression of flexible rotating links using the same distributed actuator scheme.

References

[1] Kim H-K, Choi S-B and Thompson B S 2000 Compliant control of a two-link flexible manipulator featuring piezoelectric actuators *Mech. Mach. Theory* **36** 411–24

[2] Shin H C and Choi S B 2001 Position control of a two link flexible manipulator featuring piezoelectric actuators and sensors *Mechatronics* **11** 707–29

[3] Choi S B, Cho S S, Shin H C and Kim H K 1999 Quantitative feedback theory control of a single-link flexible manipulator featuring piezoelectric actuator and sensor *Smart Mater. Struct.* **8** 338–49

[4] Sun D, Mills J K, Shan J and Tso S K 2004 A PZT actuator control of a single-link flexible manipulator based on linear velocity feedback and actuator placement *Mechatronics* **14** 1758–66

[5] Hau L C, Fung E H K and Yau D T W 2006 Multi-objective optimization of an active constrained layer damping treatment for vibration control of a rotating flexible arm *Smart Mater. Struct.* **15** 338–49
[6] Bhattacharya B, Vidyashankar B R, Patsias S and Tomlinson G R 2000 Active and passive vibration control of flexible structures using a combination of magnetostrictive and ferro-magnetic alloys *Proc. 5th European Conf. on Smart Structures and Materials*; *Proc. SPIE* **4073** 204–14
[7] Kim K J and Shahinpoor M 2003 Ionic polymer metal composites—II. Manufacturing technique *Smart Mater. Struct.* **12** 65–9
[8] Shahinpoor M, Adolf D, Segalman D and Witkowski W 1993 Electrically controlled polymeric gel actuators *US Patent Specification* 5 250 167
[9] Shahinpoor M, Bar Cohen Y, Simpson J O and Smith J 1998 Ionic polymer–metal composites (IPMC) as biomimetic sensors, actuators & artificial muscles—a review *Smart Mater. Struct.* **7** R15–30
[10] Bar-Cohen Y (ed) 2001 *Electroactive Polymer (EAP) Actuators as Artificial Muscles—Reality, Potential and Challenges* (Bellingham, WA: SPIE)
[11] Chen Z, Tan X and Shahinpoor M 2005 Quasi-static positioning of ionic polymer–metal composite (IPMC) actuators *IEEE/ASME Int. Conf. (Monterey, CA, USA, July 2005)*
[12] Shahinpoor M and Kim K J 2000 The effect of surface electrode resistance on the performance of ionic-polymer metal composite (IPMC) artificial muscles *Smart Mater. Struct.* **9** 543–51
[13] Shahinpoor M and Kim K J 2001 Ionic polymer metal composites: I. Fundamentals *Smart Mater. Struct.* **10** 819–33
[14] Shahinpoor M and Kim K J 2005 Ionic polymer–metal composites: IV. Industrial and medical applications *Smart Mater. Struct.* **14** 197–214
[15] Shahinpoor M and Kim K J 2004 Ionic polymer–metal composites: III. Modeling and simulation as biomimetic sensors, actuators, transducers, and artificial muscles *Smart Mater. Struct.* **13** 1362–88
[16] Paquette J W, Kim K W, Kim D and Yim W 2005 The behavior of ionic polymer–metal composites in a multi-layer configuration *Smart Mater. Struct.* **14** 881–8
[17] Lee D Y, Park I-S, Lee M-H, Kim K J and Heo S 2007 Ionic polymer–metal composite bending actuator loaded with multi-walled carbon nanotubes *Sensors Actuators* A **133** 117–27
[18] Kim D and Kim K J 2006 Experimental investigation on electrochemical properties of ionic polymer–metal composite *J. Intell. Mater. Syst. Struct.* **17** 449–54
[19] Bar-Cohen Y 2000 Electroactive polymers as artificial muscles—capabilities, potentials and challenges *Handbook on Biomimetics* ed Y Osada *et al* (Tokyo: NTS) section 11, chapter 8
[20] Juang J-N and Phan M Q 2001 *Identification and Control of Mechanical Systems* (Cambridge: Cambridge University Press)
[21] Wang D and Vidyasagar M 1989 Transfer functions for a single flexible link *IEEE Int. Conf. on Robotics and Automation* (Piscataway, NJ: IEEE)
[22] Bandopadhya D, Bhogadi D K, Bhattacharya B and Dutta A 2006 Active vibration suppression of a flexible link using ionic polymer metal composite *Proc. IEEE Int. Conf. CIS-RAM (Bangkok, Thailand, 7–9 June 2006)*